where T_{s1} is the available noise temperature at the output of the tuner, P_{meas} is the power measured by the NFM for each source impedance, M_{meas} is the corresponding mismatch factor for each measurement and T_o is the standard noise temperature equal to 290K. The Lane algorithm [6] is then used to extract the noise parameters from the measured noise data. The next stage of the procedure is then to insert the passive ambient DUT between the tuner and the receiver. By applying the same method as described above, the noise parameters of the whole system at the tuner reference plane are determined. The noise factor of the overall system for each source impedance point can be expressed as

$$F_{total}(\Gamma_s) = \frac{P_{meas}}{M_{meas} kGBG_{DUT} T_o} - \frac{T_{s1}}{T_o} + 1 \quad (3)$$

Using the noise parameters of the DUT/receiver cascade and the receiver exclusively in terms of their correlation matrix representations, together with the measured scattering parameters of the DUT, the correlation matrix of the DUT, and hence the noise parameters, can be deduced from eqn. 1.

Results: The factors which predominantly affect the measurement accuracy of the noise parameters include the uncertainties in the excess noise ratio calibration of the noise source, the scattering parameters of the test device and the reflection measurements of the tuner, noise source and receiver. Hence, from knowledge of these individual uncertainties, the overall measurement uncertainty of the noise parameters of the passive device could be calculated.

Table 1: Noise parameters and corresponding uncertainties of waveguide filter at 80GHz

	Noise parameters and errors			
	Errors from noise measurements		Errors from scattering parameters	
Parameter	Value	2σ	Value	2σ
F_{min} [dB]	7.707	±0.778	7.762	±0.144
R_n [Ω]	100.13	±29.58	102.47	±3.43
Γ_{opt}	0.369	±0.049	0.357	±0.004
$\angle\Gamma_{opt}$ [°]	–84.46	±7.57	–81.49	±1.014

In Table 1, both the noise parameters determined from noise measurements and the noise parameters determined directly from the scattering parameters of the waveguide filter are presented, together with the 2σ or 95% confidence of each parameter. The noise parameters show very good agreement, thus verifying the noise measurement system. The low values obtained for the uncertainties in the noise parameters F_{min}, $|\Gamma_{opt}|$ and $\angle\Gamma_{opt}$ determined from noise measurements confirm the accuracy of the values obtained. It can be seen, however, that the uncertainty R_n is large with respect to its determined value. This is because for high values of R_n, the noise factor is very sensitive to small variations in source impedance and thus results in R_n being highly sensitive to noise measurement error.

Conclusions: A fully automated noise and scattering parameter W-band measurement system and method has been demonstrated and provides a method which can also be directly applied to on-wafer measurements. The measurement system has been verified by measuring the noise parameters of a waveguide filter at 80GHz. These results show very good agreement with the noise parameters determined from scattering parameter measurements. An accurate determination of the uncertainty of each of the noise parameters has been provided. The high uncertainty value of R_n indicates this parameter to be the most sensitive to measurement error.

13 November 1997

Electronics Letters Online No: 19980090

T.A. Alam, R.D. Pollard and C.M. Snowden (*Institute of Microwaves and Photonics, School of Electronics and Electrical Engineering, University of Leeds, Leeds LS2 9JT, United Kingdom*)

References

1 BOGLIONE, L., POLLARD, R.D., POSTOYALKO, V., and ALAM, T.A.: 'Specifications for a linear network simultaneously noise and available-power matched', *IEEE Microw. Guided Lett.*, 1996, **6**, (11), pp. 407–409

2 HILLBRAND, H., and RUSSER, P.H.: 'An efficient method for computer aided noise analysis of linear amplifier networks', *IEEE Trans. Circuits Syst.*, 1976, **CAS-23**, (4), pp. 235–238

3 POSPIESZALSKI, M.W.: 'On the noise parameter of isolator and receiver with isolator at the input', *IEEE Trans. Microw. Theory Techniques*, 1986, **MTT-34**, (4), pp. 451–453

4 ADAMIAN, V., and UHLIR, A.: 'A novel procedure for receiver noise characterization', *IEEE Trans. Instrum. Meas.*, 1973, **22**, (2), pp. 181–183

5 DRURY, R., POLLARD, R.D., and SNOWDEN, C.M.: 'A 75–110 GHz automated tuner with exceptional range and repeatability', *IEEE Microw. Guided Lett.*, 1996, **6**, (10), pp. 378–379

6 LANE, R.Q.: 'The determination of device noise parameters', *Proc. IRE*, 1969, **57**, pp. 1461–1462

Direct extraction of all four transistor noise parameters from 50Ω noise figure measurements

A. Lázaro, L. Pradell, A. Beltrán and J.M. O'Callaghan

A new method for measuring the four noise parameters (NPs) of a transistor is presented. It is based on the determination of its intrinsic noise matrix elements (C_{11}^{INT}, C_{22}^{INT}, $\mathrm{Re}(C_{12}^{INT})$, $\mathrm{Im}(C_{12}^{INT})$) by fitting the measured device noise figure for a matched source reflection coefficient (F_{50}) at a number of frequency points. In contrast to previous works, no restrictive assumptions are made on the intrinsic noise sources.

Introduction: The measurement of the four noise parameters (NPs) of a transistor in the microwave frequency range is usually performed by measuring the device noise figure for a minimum of four source reflection coefficients [1 – 3] produced with a tuner [2–4]. Although this method gives accurate results [1 – 3], it has some drawbacks: (i) broadband tuners are generally very expensive and time consuming; and (ii) some tuners may have little flexibility in selecting the source coefficient patterns [2 – 5] required.

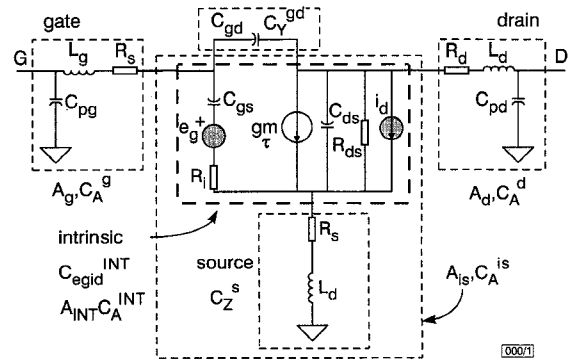

Fig. 1 *Equivalent circuit including voltage-current noise source configuration*

Other successful techniques make use of the transistor equivalent circuit as additional information to reduce complexity in the measurement procedure. In these techniques, the NPs are characterised by determining the intrinsic noise correlation matrix $[C^{INT}]$ (C_{11}^{INT}, C_{22}^{INT}, $\mathrm{Re}(C_{12}^{INT})$, $\mathrm{Im}(C_{12}^{INT})$) [6] through a number of simplifying assumptions. If the intrinsic noise sources are arranged in a voltage-current configuration (e_{gs}, i_{ds}), as shown in Fig. 1, $[C^{INT}]$ is basically frequency-independent [7 – 12]. Therefore, the intrinsic noise matrix can be obtained from a measurement of the four NPs at a single frequency, in a de-embedding procedure [10]. Furthermore, if no correlation between sources is assumed, only two frequency-independent noise constants have to be determined [7]. With additional simplifying assumptions, the four NPs can be extracted from the measurement of the device noise figure (F) at a

single frequency [8, 11], so a tuner is not required. Alternatively, Danneville *et al.* [13] have proposed a method, based in a current-current noise source configuration, in which, under a number of simplifying assumptions, the NPs are determined from a measurement of F as a function of frequency for a matched source reflection coefficient (F_{50}).

While NP determination based on F_{50} is of interest due to its simplicity, improvements in accuracy are expected if no simplifying assumptions on the intrinsic noise sources are made. The purpose of this Letter is to propose a new method to determine the intrinsic (voltage-current) transistor noise matrix, based on the measurement of F_{50} for a redundant number of frequency points, N. No restrictions are imposed on the intrinsic noise sources, in particular the correlation coefficient is not supposed to be zero, and a smooth, low-order polynomial, frequency-dependence is allowed. Experimental verification up to 26GHz is given.

Measurement and NP extraction procedure: Transistor F_{50} is measured at N frequency points in the whole range (2 – 26GHz) by a conventional technique, i.e. using a noise meter and a HOT/COLD noise source. The transistor noise figure for the measured source impedance $Z_s^i = R_s^i + jX_s^i$ (corresponding to the ith frequency) can be expressed as a function of its cascade noise matrix C_A (see Fig. 1) [6]:

$$F(Z_s^i) = 1 + \frac{1}{4kT_0\Delta f \mathrm{Re}(Z_s^i)} \cdot [1 \quad Z_s^{i*}] \cdot C_A \cdot \begin{bmatrix} 1 \\ Z_s^i \end{bmatrix} \quad (1)$$

where k is the Boltzmann constant and T_0 = 290K. According to the equivalent circuit in Fig. 1, C_A can be split into its intrinsic and extrinsic (thermal noise due to parasitic elements) contributions, $C_A = C_A^{EXT} + C_A^{INT}$, where:

$$C_A^{EXT} = C_A^g + (A_g A_{is}) C_A^d (A_g A_{is})^+ + (A_g P_{ZA}) C_Z^s (A_g P_{ZA})^+ + (A_g P_{ZA} P_{YZ}) C_Y^{gd} (A_g P_{ZA} P_{YZ})^+ \quad (2)$$

$$C_A^{INT} = P \cdot C_{e_g i_d}^{INT} \cdot P^+ \quad (3)$$

$$P = A_g P_{ZA} P_{YZ} P_{INT}, \qquad P_{INT} = \begin{bmatrix} -Y_{11}^{INT} & 0 \\ -Y_{21}^{INT} & 1 \end{bmatrix} \quad (4)$$

where (see Fig. 1) A_g, A_{is} are the ABCD matrices corresponding to the gate two-port and the series connection of the source and intrinsic two-ports, respectively, P_{ij} is the conversion matrix from i to j for the noise source configuration, and C_Z^s, C_Y^{gd} are impedance and admitance noise matrices corresponding to the source and the C_{gd} passive two-ports, respectively [6]. $C_{e_g i_d}^{INT}$ is the intrinsic voltage-current noise matrix. Note that C_A^{EXT} and $(A_g P)$ are functions of the S parameters and the room temperature only. A linear frequency dependence for the elements of C_A^{INT} is assumed ($C_{ij}^{INT} = C_{ij}^0 + C_{ij}^1 \cdot f$), although higher order polynomials have also been considered with no significant improvement in results. Substituting eqns. 2 – 4 into eqn. 1, the following overdetermined linear equation system is obtained for $C_{e_g i_d}^{INT}$:

$$[y_i] = [M] \cdot [X] \qquad i = 1, \ldots, N \quad (5)$$

$$y_i = 4kT_0\Delta f \cdot (F(Z_s^i) - 1) \cdot \mathrm{Re}Z_s^i - [1 \quad Z_s^{i*}] \cdot C_A^{EXT} \cdot [1 \quad Z_s^i]^T \quad (6)$$

$$M_{i1} = |P_{11}|^2 + |Z_s^i|^2 |P_{21}|^2 + 2R_s^i \mathrm{Re}(P_{11}P_{21}^*) - 2X_s^i \mathrm{Im}(P_{11}P_{21}^*) \quad (7)$$

$$M_{i2} = |P_{12}|^2 + |Z_s^i|^2 |P_{22}|^2 + 2R_s^i \mathrm{Re}(P_{12}P_{22}^*) - 2X_s^i \mathrm{Im}(P_{12}P_{22}^*) \quad (8)$$

$$M_{i3} = 2\mathrm{Re}(P_{11}P_{12}^*) + 2|Z_s^i|^2 \mathrm{Re}(P_{12}P_{22}^*) + 2R_s^i \mathrm{Re}(P_{12}P_{21}^* + P_{11}P_{22}^*) \quad (9)$$

$$M_{i4} = -2\mathrm{Im}(P_{11}P_{12}^*) - 2|Z_s^i|^2 \mathrm{Im}(P_{21}P_{22}^*) - 2R_s^i \mathrm{Re}(P_{11}P_{21}^* - P_{12}P_{22}^*) \quad (10)$$

where $[X] = [C^0] + [f_i][C^1]$, $[C^k] = [C_{11}^k, C_{22}^k, \mathrm{Re}C_{12}^k, \mathrm{Im}C_{12}^k]^T$, k = 0, 1.

The fitting procedure begins, assuming no frequency dependence on C_{ij}^{INT} ($C_{ij}^1 = 0$), and the equation system of eqn. 5 is solved for $C_{e_g i_d}^{INT}$ by least squares using pseudo-inverse calculation. The values obtained for C_{ij}^0 are used as initial values in a simplex algorithm that estimates C_{ij}^0 and C_{ij}^1 for the best fit of the computed F_{50} (eqns. 5 – 10) to the measured F_{50}.

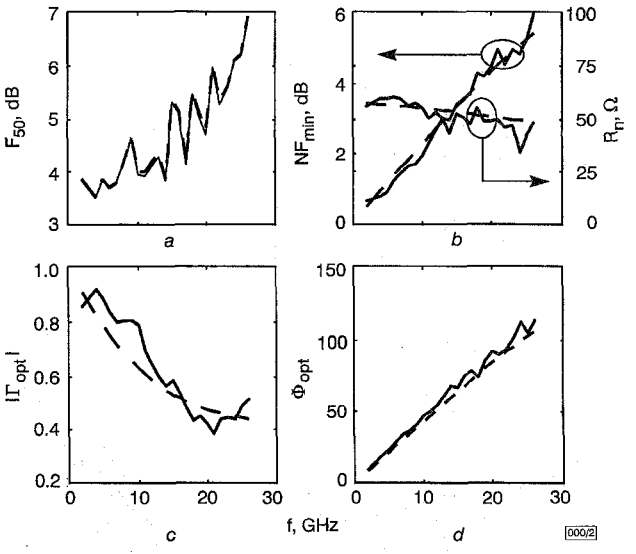

Fig. 2 *Experimental results for 0.3μm gate length HEMT*

a Comparison of F_{50}
——— measured
– – – – computed from NPs measured with new technique
b–d Comparison of NPs
——— measured directly using commercial system [4]
– – – – measured with the new technique

Experimental results: The method has been tested on on-wafer 0.3μm HEMTs from the FhG-IAF DPD-SQW process. Fig. 2*a* compares the computed F_{50} to the measured F_{50} up to 26GHz, showing an excellent agreement, within a measurement accuracy (including noise meter and noise source) of about ±0.14dB RSS. C_{11}^{INT} is a constant, and $\mathrm{Im}(C_{12}^{INT})$ is very small and almost constant (one order of magnitude smaller than $\mathrm{Re}(C_{12}^{INT})$), as suggested in the literature [7, 9, 10]. For these particular devices, the best fitting of F_{50} has been obtained when $\mathrm{Re}(C_{12}^{INT})$ is not neglected and a frequency slope is allowed for $\mathrm{Re}(C_{12}^{INT})$ and C_{22}^{INT}. These results also agree with the literature [7]. In Fig. 2*b–d*, the transistor NPs computed from the measured noise matrix are compared to the NPs directly measured using a commercial system [4] based on a broadband tuner, also showing an excellent agreement.

Conclusions: A mathematical method for determining the noise matrix $C_{e_g i_d}^{INT}$ of FBTs based on the measurement of F_{50} for a redundant number of frequency points has been proposed and successfully applied to HEMTs. By assuming a smooth frequency dependence for the elements of $C_{e_g i_d}^{INT}$, excellent agreement between the computed F_{50} and the measured F_{50} up to 26GHz is achieved. The noise matrix elements obtained, and their frequency dependence, agree with results previously published by other authors. Enhanced accuracy is obtained if $\mathrm{Re}(C_{12}^{INT})$ is not neglected.

Acknowledgment: This work has been supported by the research project TIC-672-C04-03/93 financed by the Spanish CICYT.

23 October 1997
Electronics Letters Online No: 19980192

A. Lázaro, L. Pradell, A. Beltrán and J.M. O'Callaghan (*Polytechnic University of Catalunya (UPC), Dept. TSC, Campus Nord UPC, 08034 Barcelona, Spain*)

References

1 LANE, R.Q.: 'The determination of device noise parameters', *Proc. IEEE*, 1969, **57**, pp. 1461–1462

2 SANNINO, M.: 'On the determination of device noise and gain parameters (of linear two-ports)', *Proc. IEEE*, 1979, **67**, (9), pp. 1364–1366

3 DAVIDSON, A.C., LEAKE, B.W., and STRID, E.: 'Accuracy improvements in microwave noise parameter measurements', *IEEE Trans. Microwave Theory Tech.*, 1989, **37**, (12), pp. 1973–1978
4 NPTS-26 System, Cascade-Microtech, Inc., 14255 SW Brigadoon, Beaverton, OR 97005
5 O'CALLAGHAN, J.M., ALEGRET, A., PRADELL, L., and CORBELLA, I.: 'Ill conditioning loci in noise parameter determination', *Electron. Lett.*, 1996, **32**, (18), pp. 1680–1681
6 HILLBRAND, H., and RUSSER, P.R.: 'An efficient method for computer aided noise analysis of linear amplifier networks', *IEEE Trans. Circuits Syst.*, 1976, **23**, (4), pp. 235–238
7 POSPIESZALSKI, M.: 'Modeling of noise parameters of MESFET's and MODFET's and their frecuency and temperature dependence', *IEEE Trans. Microwave Theory Tech.*, 1989, **37**, (9), pp. 1340–1350
8 TASKER, P.J., REINERT, W., HUGHES, B., BRAUNSTEIN, J., and SCHLECHTWEG, M.: 'Direct extraction of all four transistor noise parameters using a 50Ω measurement system'. IEEE MTT-S Int. Microwave Symp., 1993,
9 DANNEVILLE, F., HAPPY, H., DAMBRINE, G., BELQUIN, J., and CAPPY, A.: 'Microscopic noise modeling and macroscopic noise models: How good a connection?', *IEEE Trans. Electron Devices*, 1994, **41**, (5), pp. 779–785
10 PUCEL, R.A.: 'A general noise de-embedding procedure for packaged two-port linear active devices', *IEEE Trans. Microwave Theory Tech.*, 1992, **40**, (11), pp. 2013–2020
11 GUPTA, M.S., and GREILING, P.T.: 'Microwave noise characterization of GaAs MESFET's, determination of extrinsic noise parameters', *IEEE Trans. Microwave Theory Tech.*, 1988, **36**, (4), pp. 745–751
12 GASMI, A., RUYART, B., BERGEAULT, E., and JALLET, L.P.: 'A new calculation approach of transistor noise parameters as a function of gatewidth and bias current', *IEEE Trans. Microwave Theory Tech.*, 1997, **45**, (3), pp. 338–344
13 DAMBRINE, G., HAPPY, H., DANNEVILLE, F., and CAPPY, A.: 'A new method for on wafer noise measurement', *IEEE Trans. Microwave Theory Tech.*, 1993, **41**, (3), pp. 375–381

Discrepancies obtained in transconductance extracted from pulsed I-V curves and from pulsed S-parameters in HEMTs and PHEMTs

J.M. Collantes, Z. Ouarch, C.-Y. Chi, M. Sayed and R. Quere

An isothermal comparison between the transconductance extracted from S-parameter measurements (*gm_RF*) and the transconductance derived from I-V curves (*gm_IV*) is performed for HEMT and PHEMT transistors. The isothermal environment is achieved by carrying out a complete pulse characterisation (pulsed I-V and pulsed S-parameters) that avoids the effects of self-heating. Results show a *gm_RF* that can be > 40% larger than *gm_IV* at high V_{gs} voltages. Thermal effects are avoided during the pulsed characterisation, therefore this discrepancy is attributed to fast traps.

Introduction: HEMT and PHEMT transistors play a major role in today's microwave- and millimetre-wave electronics. MMICs of these technologies are commonly used in a wide range of commercial applications, such as phased-array antennas, digital personal communications, automotive anti-collision radar, WLAN, etc. Therefore, designers need accurate models to reduce the development cycle and to lower manufacturing costs. These models require accurate and consistent extraction and characterisation procedures. It is already well-known that traditional DC characterisation is not well suited to accurate nonlinear model extraction since self-heating and trapping effects perturb the measurements and give rise to low-frequency dispersion of conductance and transconductance [1, 2]. To overcome these problems, pulsed characterisation systems have recently been developed. In these systems, the device I-V curves are measured by applying very narrow pulses (1 μs or lower) with very low duty cycles. If the pulse width is shorter than the thermal and trapping time constants, the characterisation can be performed under isothermal and isotrapping conditions. In addition, some pulsed systems allow the measurement of the device scattering parameters by superimposing an RF small-signal on top of the DC pulse voltage. This provides a completely consistent characterisation of the device in which both DC and RF measurements are performed under pulsed conditions.

If isothermal and isotrapping conditions are accomplished during the pulsed characterisation, the transconductance obtained from the pulsed I-V curves (*gm_IV*) must be consistent with that extracted from the pulsed S-parameters (*gm_RF*). This consistency has already been proved in MESFET and MOSFET devices [3, 4]. In this Letter, we compare the *gm_IV* obtained from pulsed I-V curves with the *gm_RF* extracted from pulsed S-parameters for HEMT and PHEMT devices. Results will show that strong discrepancies appear between them at high V_{gs} values. Since self-heating effects are avoided during characterisation, this discrepancy must be caused by trapping time constants shorter than the duration of the applied pulses.

Experimental results from commercial PHEMTs (from two different foundries) and HEMTs are presented in this analysis. For each type of device, the measurements have been performed on a large number of samples, from a variety of wafers. Similar results have been obtained in all instances; this ensures that the conclusions extracted here are of a general nature.

Measurement systems: Pulsed I-V and pulsed S-parameter characterisations have been performed with two different pulsed measurement systems, developed at the IRCOM-Limoges University (France) [3] and by Hewlett-Packard [5]. Both systems can provide a pulsed I-V and pulsed S-parameter characterisation of the device under test using very narrow pulses (narrower than 1 μs). PHEMT devices from the first foundry were characterised with the HP system, and PHEMTs from the second foundry were characterised with the IRCOM system. The characterisation of the HEMT devices was carried out in both systems. The pulsed I-V curves and pulsed S-parameters of the HEMT transistors obtained from the two systems show differences of < 3%. This ensures that the results of the analysis are consistent and are not distorted by measurement uncertainties.

Pulsed characterisation: All of the devices are characterised by pulses of 600ns in length and a duty cycle of 10%. These values ensure that the device temperature is kept constant during the characterisation. On the one hand, 600ns is significantly lower than the thermal constant of the devices; on the other hand, measurements with lower duty cycles were performed, obtaining similar I-V curves, implying that a duty cycle of 10% provides isothermal results for these devices. Therefore, we can ensure that the characterisation is performed under isothermal conditions. S-parameters are measured under pulsed conditions all over the ranges of V_{gs} and V_{ds} values from 1 to 10GHz.

Transconductance extraction: The comparison between *gm_RF* and *gm_IV* will be performed on extrinsic values referred to the ports of the device so that the results will not be perturbed by errors occurring in the extraction of the extrinsic parameters of the device, especially by errors in the determination of the source resistance R_s. To obtain the extrinsic *gm_RF*, we transform the measured S-parameters into Y-parameters, and then calculate the extrinsic *gm_RF* by extrapolating at zero frequency the magnitude of Y21 measured at low frequencies. The extrinsic *gm_IV* is computed from increments of the measured pulsed I-V curves ($gm = dI_{ds}/dV_{gs}$) using very small δV_{gs}.

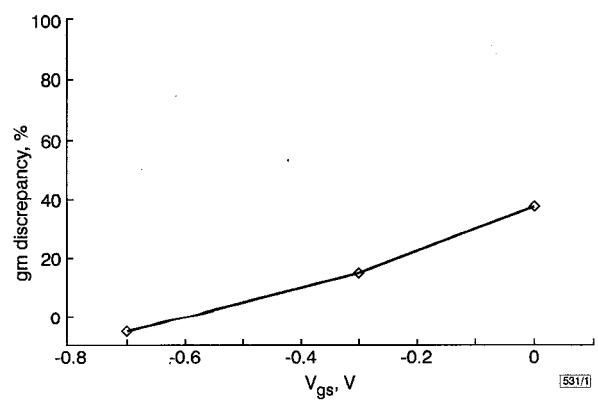

Fig. 1 *gm discrepancy obtained for PHEMT from first foundry, measured with HP pulse system*

V_{ds} = 6V